Optica Applicata, Vol. XXXVI, No. 1, 2006

Efficient residual error reduction in complex spectral optical coherence tomography with arbitrary or unknown phase

MACIEJ SZKULMOWSKI*, TOMASZ BAJRASZEWSKI, ANNA SZKULMOWSKA, PIOTR TARGOWSKI, ANDRZEJ KOWALCZYK

Institute of Physics, Nicolaus Copernicus University,
ul. Grudziądzka 5/7, 87-100 Toruń, Poland

*Corresponding author: M. Szkulmowski, szkulik@fizyka.umk.pl

Complex spectral optical coherence tomography (CSOCT) produces images free of parasitic mirror components. This effectively doubles the measurement range. Complete removal of mirror components from CSOCT tomograms requires exact knowledge of the phase shifts introduced, which is usually difficult to achieve. The method presented effectively removes the mirror image, even without precise knowledge of the phases and is applicable to any variation of CSOCT. "Mirror-image-free" tomograms of a human anterior chamber *in vivo* obtained with the aid of this approach are presented.

Keywords: optical coherence tomography (OCT), spectral interferometry, complex spectral optical coherence tomography (CSOCT), numerical data analysis.

1. Introduction

Optical coherence tomography (OCT) is a well-established, optical interferometric method used in medical imaging. The method analyses back-scattering of light from an object penetrated by a beam of low temporal but high spatial coherence. As a result, the in-depth scattering profile of the object investigated is obtained. There are two implementations of OCT. Historically, the first was time-domain OCT (TdOCT), whereas the second – so-called spectral OCT (SOCT) – was developed rather later.

In TdOCT [1], a single in-depth scattering profile is obtained by changing the light path in the reference arm of the interferometer. In such a system, both the depth and transversal directions have to be scanned mechanically in order to register a two-dimensional cross-sectional map of the region of interest within the object. The method has successfully been applied for visualization of retinal and corneal anatomy and pathology [2–5], as well as for dermal [6] and gastroenterological

imaging [7]. It has also been implemented commercially (StratusOCT – Carl Zeiss Meditech Inc., OCT-Ophthalmoscope – Ophthalmic Technologies Inc.).

An alternative to TdOCT is spectral optical coherence tomography (SOCT) [8, 9]. This is about 100-fold faster and significantly more sensitive [10–14] than traditional time-domain OCT, which makes it particularly useful in ophthalmology [9, 10, 15]. In SOCT, light leaving the interferometer is analysed by a spectrometer and detected as a function of wavelength by a CCD camera. The image reconstruction is performed via Fourier transformation of recorded spectra. As the spectrum is real, its Fourier transform contains two "mirror-reversed" images. In order to obtain a useful tomogram, the two images should not overlap. For thin objects (like the retina of the eye), this is achieved by separating the images in Fourier space. Unfortunately, this simple procedure halves the imaging range, making the SOCT method difficult to apply to imaging of thick objects, such as the anterior chamber of the eye.

The full available imaging range is attained if the Fourier transformation is applied to the complex interferometric signal. The phase information required to reconstruct such a signal from intensity measurements is obtained from recordings of two to five spectra collected for a constant penetrating beam, but with the reference mirror being shifted by various fractions of wavelength of the light used [16–19]. The phase shift can also be introduced by using a reference beam with a tilted wavefront [20], or by optic couplers [21]. These methods are called complex spectral optical coherence tomography (CSOCT). If the complex signal is precisely recovered, its Fourier transform is free of the "mirror" component.

In practice, such a result is difficult to achieve. Most of the methods [16–18] require shifting the reference mirror by a precise fraction of the wavelength. If a relatively broadband light source is used, this leads to so-called polychromatic error, since this condition is fulfilled for one wavelength only. We have overcome this drawback with an algorithm calculating phase shifts for every wavelength from known mirror displacements [19]. Even this method is not sufficient for *in vivo* measurements, since involuntary movements of the eye examined introduce phase noise, leading to residual "mirror-reversed" images ("ghosts"). This effect may be eliminated numerically by fine adjustments of the phases used to recover the complex signal [22]. This procedure is effective, although it requires significant computation time.

In this contribution, we present a simple and fast method avoiding these disadvantages which can be used to remove faint mirror images in any kind of CSOCT tomogram.

2. Theory

The interferometric component retrieved from the whole signal registered by SOCT spectrography can be expressed as follows:

$$G'(k) = S(k)\sum_j 2\sqrt{I_R I_j}\cos(kz_j) \tag{1}$$

where $S(k)$ is the spectrum of the light source, I_R is the intensity of returning light in the reference arm of the interferometer, I_j is the intensity of scattered light returning from the j-th reflecting interface inside the sample, and z_j is the optical path difference between the light reflected from the mirror in the reference arm and the light scattered at the j-th interface in the sample. Since the mirror is held in fixed position, these numbers are equivalent to the positions of the scattering interfaces. Other components of the SOCT signal (useless for SOCT analysis and not appearing in Eq. (1)) are effectively removed by numerical procedures, described in detail in [23].

In order to recover positions z_j, one has to calculate the Fourier transform of $G'(k)$

$$g(z) = \mathrm{FT}(G'(k)) = s(z) \otimes \sum_j 2\sqrt{I_R I_j}\,\delta(z \pm z_j) \tag{2}$$

where $s(z)$ is the Fourier transform of $S(k)$ and $\otimes$ denotes convolution. The above expression describes several peaks located at the positions of the scattering interfaces convolved with $s(z)$. Unfortunately in Eq. (2) every interface in the sample shows up twice at two different locations ($z \pm z_j$). Due to this fact, SOCT tomograms always comprise two "mirror-reversed" images. In order to achieve the full possible imaging range, it is necessary to create a complex interferometric signal, instead of a real one (Eq. (1)):

$$G''(k) = S(k)\sum_j 2\sqrt{I_R I_j}\,\exp(ikz_j) \tag{3}$$

Several methods have so far been proposed to achieve this goal. All of them require a number of additional measurements conducted in the same place in the sample with phase shift introduced in the reference arm. The methods work well only when the shifts are set to integral numbers of $\lambda/2n$ for n shifts, or the exact values of arbitrary shifts are known. Otherwise, one of the images is not completely removed, and a faint "ghost" remains. In this contribution, we propose a two-step procedure to eliminate the "ghost" mirror image.

In the first step, one of the mirror images must be suppressed as much as possible in order to introduce asymmetry in the image. Sufficient suppression occurs in all of the known CSOCT methods to fulfil this condition.

In the second step, every line of the tomogram (A-scan) obtained in the first step is reversed and, after scaling, subtracted from the original A-scan. The scaling factor f is calculated from intensities of peaks that are well isolated:

$$f = \frac{I_G - I_N}{I_M - I_N} \tag{4}$$

where I_M, I_G, I_N are the intensities of the main image, the "ghost" image and the background noise level, respectively.

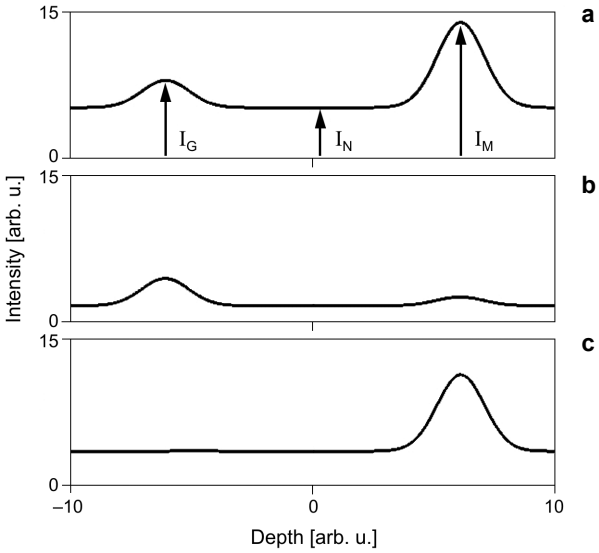

Fig. 1. Schematic of the second step of the proposed method. **a** – an A-scan obtained via Fourier transformation of complex interferometric signal (see Eq. (3)). This procedure introduces asymmetry of intensity magnitudes in the main (I_M) and 'mirror-reversed' (I_G) images. The background noise level is labeled I_N. **b** – the scaled (Eq. (4)) and reversed A-scan from (**a**). **c** – the effect of subtraction of (**b**) from (**a**).

The method is computationally effective, as it consists only of a few multiplications and subtractions. The total procedure is presented in a pictorial way in Fig. 1.

The scaling factor f is computed separately for every A-scan. In practice, f is calculated by minimaization of a fuction $R(f)$:

$$R(f) = \sum_n V_n V_{N-n}$$

$$V_k = |A_k - f A_{N-k}|$$

where A_k is the intensity at the k-th point of a smoothed A-scan obtained with complex method, A_{N-k} is the intensity in its mirror image, and the function $R(f)$ represents the level of correlation between the clean A-scan V_n and its mirror image V_{N-n}. The function $R(f)$ reaches minimum if the ghosts are completely suppressed.

The main drawback of the method is a slight decrease in the signal-to-noise ratio. The signal-to-noise ratio of the main image before applying the method is given by:

$$\left(\frac{S}{N}\right)_{\text{uncorr}} = \frac{I_M - I_N}{\sigma} \tag{5}$$

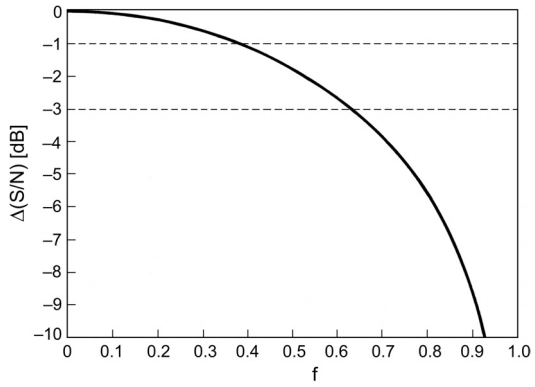

Fig. 2. Decrease of the signal-to-noise ratio of the CSOCT tomogram after applying the "ghost" image reduction technique, as a function of the scaling factor f (Eq. (7)). The dashed lines show the –1 and –3 dB levels.

where σ is the variance of the noise. After applying the method, the signal-to-noise ratio decreases, and can be described as:

$$\left(\frac{S}{N}\right)_{\text{corr}} = \frac{I_M - fI_G - I_N(1-f)}{\sigma\sqrt{1+f^2}} \tag{6}$$

The above equation may be rewritten in the more convenient form:

$$\left(\frac{S}{N}\right)_{\text{corr}} = \left(\frac{S}{N}\right)_{\text{uncorr}} \frac{1-f^2}{\sqrt{1+f^2}} \tag{7}$$

The value of $(S/N)_{\text{corr}}$ is a function of the scaling factor f, see Fig. 2.

In order to obtain a high signal-to-noise ratio, one should try to attain as great an intensity difference between the main image and the "ghost" as possible. It can however be seen that even when the scaling factor f is equal to 0.4, the decrease of the signal-to-noise ratio is only about 1 dB. Because the signal-to-noise ratio achievable by the SOCT technique is about 90 dB, [24] and tomograms are plotted on a logarithmic scale, this decrease of signal-to-noise ratio does not noticeably affect image quality.

In order for the method to work properly, "mirror-reversed" images may differ only in amplitude: the shapes of the two images (defined by $s(z)$, Eq. (2)) have to be identical. If this is not the case, simple subtraction does not remove the "ghost" image. Therefore, the method cannot be applied to CSOCT tomograms if numeric dispersion compensation has been applied [14].

3. Results and discussion

All results have been obtained with our in-house SOCT instrument based on an optical fiber Michelson interferometer set-up (Fig. 3). The superluminescent diode with high spatial, but low temporal coherence is used as a light source (Superlum, Russia, central wavelength 811 nm, full width at half maximum 20 nm). The light is split by the fiber coupler into reference and object arms. The mirror in the reference arm is fixed to the piezotranslator (Physik Instrumente, Germany), which enables introduction of preselected delays. The object arm consists of a collimator, transversal scanners and custom designed interface optics, which allows for imaging the anterior part of the eye. The narrow beam of light penetrates the object, scatters from the elements of its structure, then is collected by the same optics back to the coupler. Then, it interferes with the light returning from the reference arm and the spectrum of the interference signal is detected by a 12-bit line scan CCD camera and transferred to a personal computer.

In the work reported in this contribution, we used a two-frame method [18]. In this approach, two spectra $G_1(k)$ and $G_2(k)$, taken at the same point of the object, are combined into a complex signal using the following relationship:

$$G'(k) = G_1(k) + i\,G_2(k) \tag{8}$$

The modulus of the inverse Fourier transform of $G'(k)$ gives a "ghost"-free tomogram providing the phase shift between $G_1(k)$ and $G_2(k)$ is exactly equal to $\pi/2$ for every k and the phase error remains small. We tested a case where these conditions were deliberately not fulfilled – for a phase shift between the two measurements set to $2\pi/3$, so that a faint "ghost" image was present in the tomogram.

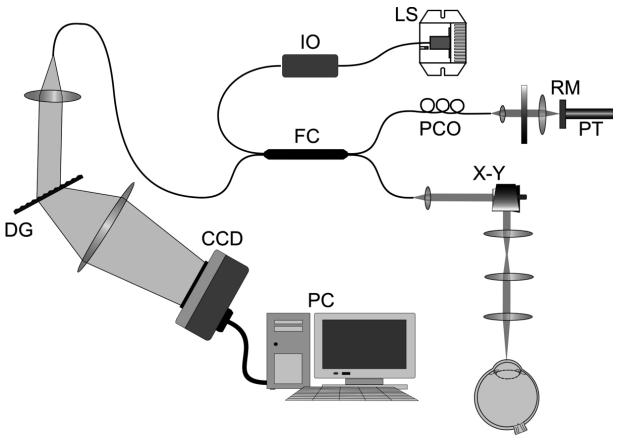

Fig. 3. Diagram of the instrument: LS – superluminescent light source, IO – fiber isolator, FC – fiber coupler, PCO – polarization controller, RM – reference mirror, PT – piezotranslator, X-Y – galvoscanners, DG – diffraction grating, CCD – line scan camera, PC – personal computer.

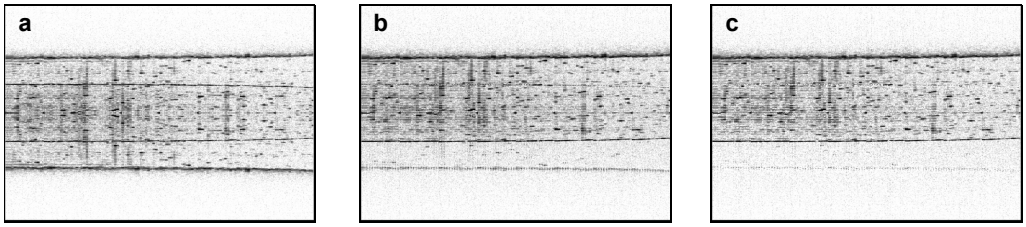

Fig. 4. Immobile phantom probe. Classical SOCT tomogram with overlapping mirror images (**a**). The CSOCT tomogram with visible "ghost" image (**b**). Final image with "ghost" suppressed (**c**).

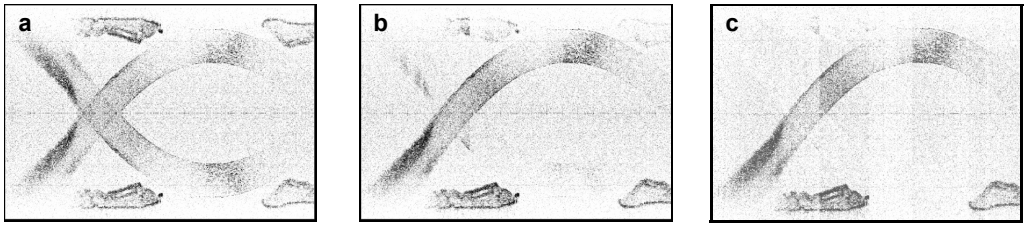

Fig. 5. Human anterior chamber *in vivo*. Classical SOCT tomogram with overlapping mirror images (**a**). The CSOCT tomogram with visible "ghost" image (**b**). Final image with "ghost" suppressed (**c**).

To investigate the potential of the method, we analysed an immobile phantom probe (a roll of adhesive transparent tape, Fig. 4), and the anterior chamber of a human volunteer (Fig. 5). In both cases, two spectra for one line of a tomogram (A-scan) were acquired with mirror displacement of about 130 nm between the measurements. The complex signal was generated according to Eq. (8). Then the second step of the proposed method was performed. The average value of the scaling factor in both cases was equal to 0.43, which gives a decrease in signal-to-noise ratio of about 1.3 dB.

In Figures 4 and 5, the tomograms obtained at different stages of processing are presented. Panels 4**a** and 5**a** show the results of the classical SOCT method. Both mirror images have the same intensity. The images obtained after applying the first and the second steps of the procedure are presented in panels **b** and **c**, respectively. In panels **b**, application of the complex method leads to suppression of one of the images, and introduces asymmetry in the image, thus enabling the application of the second step of our method. In panels **c**, these residual "ghosts" are further suppressed by subtraction of the scaled mirror image, as described above.

4. Conclusions

The proposed method is fast, and its capability of removing "ghost" residual images from CSOCT tomograms is satisfactory. It can be used in cases where the phase shift is unknown or is unstable, which conditions preclude the application of standard

CSOCT techniques. The price to be paid is a slight decrease in the signal-to-noise ratio. The method cannot be applied together with numeric dispersion compensation.

Acknowledgement – This work was supported by the Polish State Committee for Scientific Research (KBN) under grant KBN 4T11E02322.

References

[1] HUANG D., SWANSON E.A., LIN C.P., SCHUMAN J.S, STINSON W.G., CHANG W., HEE M.R., FLOTTE T., GREGORY K., PULIAFITO C.A., FUJIMOTO J.G., *Optical coherence tomography*, Science **254**(5035), 1991, pp. 1178–81.

[2] HEE M.R., IZATT J.A., SWANSON E.A., HUANG D., SCHUMAN J.S., LIN C.P., PULIAFITO C.A., FUJIMOTO J.G., *Optical coherence tomography of the human retina*, Archives of Ophthalmology **113**(3), 1995, pp. 325–32.

[3] PULIAFITO C.A., HEE M.R, LIN C.P., REICHEL E., SCHUMAN J.S., DUKER J.S., IZATT J.A., SWANSON E.A., FUJIMOTO J.G., *Imaging of macular diseases with optical coherence tomography*, Ophthalmology **102**(2), 1995, pp. 217–29.

[4] DREXLER W., MORGNER U., GHANTA R.K., KÄRTNER F.X., SCHUMAN J.S., FUJIMOTO J.G., *Ultrahigh -resolution ophthalmic optical coherence tomography* Nature Medicine **7**(4), 2001, pp. 502–7, [erratum appears in Nat. Med. **7**(5), 2001, p. 636].

[5] DREXLER W., SATTMANN H., HERMANN B., KO T.H., STUR M., UNTERHUBER A., SCHOLDA C., FINDL O., WIRTITSCH M., FUJIMOTO J.G., FERCHER A.F., *Enhanced visualization of macular pathology with the use of ultrahigh-resolution optical coherence tomography*, Archives of Ophthalmology **121**(5), 2003, pp. 695–706.

[6] WELZEL J., *Optical coherence tomography in dermatology: a review*, Skin Research and Technology **7**(1), 2001, pp. 1–9.

[7] ROLLINS A.M., UNG-ARUNYAWEE R., CHAK A., WONG R.C.K., KOBAYASHI K., SIVAK M.V., IZATT J.A., *Real-time in vivo imaging of human gastrointestinal ultrastructure by use of endoscopic optical coherence tomography with a novel efficient interferometer design*, Optics Letters **24**(19), 1999, pp. 1358–60.

[8] FERCHER A.F., HITZENBERGER C.K., KAMP G., EL-ZAIAT S.Y., *Measurement of intraocular distances by backscattering spectral interferometry*, Optics Communications **117**(1–2), 1995, pp. 43–8.

[9] WOJTKOWSKI M., LEITGEB R., KOWALCZYK A., BAJRASZEWSKI T., FERCHER A.F., *In vivo human retinal imaging by Fourier domain optical coherence tomography*, Journal of Biomedical Optics **7**(3), 2002, pp. 457–63.

[10] WOJTKOWSKI M., BAJRASZEWSKI T., TARGOWSKI P., KOWALCZYK A., *Real-time in vivo imaging by high-speed spectral optical coherence tomography*, Optics Letters **28**(19), 2003, pp. 1745–7.

[11] LEITGEB R., HITZENBERGER C.K., FERCHER A., *Performance of fourier domain vs. time domain optical coherence tomography*, Optics Express **11**(8), 2003, pp. 889–94.

[12] DE BOER J.F., CENSE B., PARK B.H., PIERCE M.C., TEARNEY G.J., BOUMA B.E., *Improved signal-to -noise ratio in spectral-domain compared with time-domain optical coherence tomography*, Optics Letters **28**(21), 2003, pp. 2067–9.

[13] CHOMA M.A., SARUNIC M.V., YANG C.H., IZATT J., *Sensitivity advantage of swept source and Fourier domain optical coherence tomography*, Optics Express **11**(18), 2003, pp. 2183–9.

[14] WOJTKOWSKI M., SRINIVASAN V.J., KO T.H., FUJIMOTO J.G., KOWALCZYK A., DUKER J.S., *Ultrahigh -resolution, high-speed, Fourier domain optical coherence tomography and methods for dispersion compensation*, Optics Express **12**(11), 2004, pp. 2404–22.

[15] NASSIF N.A., CENSE B., PARK B.H., PIERCE M.C., YUN S.H., BOUMA B.E., TEARNEY G.J., CHEN T.C., DE BOER J.F., *In vivo high-resolution video-rate spectral-domain optical coherence tomography of the human retina and optic nerve*, Optics Express **12**(3), 2004, pp. 367–76.

[16] WOJTKOWSKI M., KOWALCZYK A., LEITGEB R., FERCHER A.F., *Autocorrelation free spectral OCT techniques in eye imaging*, Proceedings of the SPIE **4431**, 2001, pp. 46–51.
[17] WOJTKOWSKI M., KOWALCZYK A., LEITGEB R., FERCHER A.F., *Full range complex spectral optical coherence tomography technique in eye imaging*, Optics Letters **27**(16), 2002, pp. 1415–7.
[18] LEITGEB R., BAJRASZEWSKI T., HITZENBERGER C.K., FERCHER A.F., *Novel phase-shifting algorithm to achieve high-speed long-depth range probing by frequency domain optical coherence tomography*, Proceedings of the SPIE **4956**, 2003, pp. 101–8.
[19] TARGOWSKI P., WOJTKOWSKI M., KOWALCZYK A., BAJRASZEWSKI T., SZKULMOWSKI M., GORCZYNSKA I., *Complex spectral OCT in human eye imaging in vivo*, Optics Communications **229**(1–6), 2004, pp. 79–84.
[20] YASUNO Y., MAKITA S., ENDO T., AOKI G., SUMIMURA H., ITOH M., YATAGI T., *One-shot-phase -shifting Fourier domain optical coherence tomography by reference wavefront tilting*, Optics Express **12**(25), 2004, pp. 6184–91.
[21] CHOMA M.A., YANG C., IZATT J.A., *Instantaneous quadrature low-coherence interferometry with 3*3 fiber-optic couplers*, Optics Letters **28**(22), 2003, pp. 2162–4.
[22] TARGOWSKI P., GORCZYŃSKA I., SZKULMOWSKI M., WOJTKOWSKI M., KOWALCZYK A., *Improved complex spectral domain OCT for in vivo eye imaging*, Optics Communications **249**(1–3), 2005, pp. 357–62.
[23] SZKULMOWSKI M., WOJTKOWSKI M., BAJRASZEWSKI T., GORCZYŃSKA I., TARGOWSKI P., WASILEWSKI W., KOWALCZYK A., RADZEWICZ C., *Quality improvement for high resolution in vivo images by spectral domain optical coherence tomography with supercontinuum source*, Optics Communications **246**(4–6), 2005, pp. 569–78.
[24] SZKULMOWSKA A., WOJTKOWSKI M., GORCZYŃSKA I., BAJRASZEWSKI T., SZKULMOWSKI M., TARGOWSKI P., KOWALCZYK A., KAŁUŻNY J.J., *Coherent noise-free ophthalmic imaging by spectral optical coherence tomography*, Journal of Physics D: Applied Physics **38**(15), 2005, pp. 2606–11.

Received June 23, 2005
in revised form August 29, 2005